1 The relationship between self-diffusion activation

2 energy and Soret coefficient in binary liquid mixtures

- 3 Micah Silverman, Daniel Hallinan Jr.
- 4 Aero-propulsion, Mechatronics, and Energy Center, Florida A&M University–Florida State
- 5 University College of Engineering, Tallahassee, FL 32310
- 6 Chemical and Biomedical Engineering, Florida A&M University–Florida State University
- 7 College of Engineering, Tallahassee, FL 32310

8 Abstract

- 9 The Soret effect is an observed phenomenon in which an applied temperature gradient
- will induce a concentration gradient in multicomponent mixtures. The Soret coefficient is
- the ratio of thermally driven diffusion to mutual diffusion driven by concentration gradients.
- 12 It is measured at steady state when the two driving forces are balanced, i.e. the net flux
- is zero. This study is designed to explore the potential relationship between the activation
- 14 energy of self-diffusion of the individual components of a binary mixture and the mixture's
- 15 resulting Soret coefficient. This study found a trend of increasingly negative Soret
- 16 coefficients as the difference in the mole-fraction-weighted self-diffusion activation
- 17 energies of the components increased.
- 18 **Keywords:** Thermal Diffusion, Self-Diffusion Coefficient, Empirical Relations,
- 19 Temperature Gradient, Concentration Gradient

21 Introduction

22

23

24

25

26

27

28

29

30

31

32

33

34

35

36

37

38

39

40

41

42

43

44

45

The Soret effect, whereby a concentration gradient forms when a multi-component mixture is exposed to a temperature gradient, is experimentally well-established.(Platten et al., 2003) The Soret effect has tremendous potential to be used in several energy harnessing capacities. The most promising of these is waste heat energy recapture. Wasted heat energy is a major issue with 70% of all energy produced being lost as heat waste. (Jones, 2018) This astounding figure is why waste energy recapture has become one of the most intriguing concepts in energy today. Our approach to addressing this issue is through the development of our understanding of the Soret effect. The long-term potential of this work is to develop a reusable polymer-electrolyte thermogalvanic cell, which could generate electricity like a battery but driven by thermal rather than chemical potential gradients. (Mentor et al., 2020) It would do this by using waste heat energy as a heat source and atmospheric conditions as a heat sink to create the temperature gradient previously mentioned. This would mean that wasted energy could be recaptured with a simple thermogalvanic cell, making it a cost-effective and accessible form of energy. (Yu et al., 2019) In addition to industrial processes, this work also has the potential to be harnessed for use in cars (exhaust heat) and other consumer products, as well as potentially with geothermal applications(Vining, 2009) and to improve the efficiency of other power generation systems. Study of the Soret Effect has a long empirical and phenomenological history. The earliest studies, by Ludwig and Soret, used aqueous electrolytes. In the early 1900's, significant emphasis was placed on studying gas mixtures, (Grew and lbbs, 1952) due to the simplicity of molecular interactions in such systems and therefore the ability to model thermal diffusion with kinetic gas theory.(Hirschfelder et al., 1954) More recently, studies have been motivated by the practical significance of the experimental system. In an attempt to understand the behavior of petrochemicals in geological deposits, much work has been done on liquid hydrocarbon mixtures, (Köhler and Morozov, 2016) which are the focus herein. In the past two decades,

polymer solutions and polymer blends have been studied, primarily to better understand the success of thermal flow field fractionation for the separation of polyolefins(Malik and Pasch, 2016; Messaud et al., 2009; VanBatten et al., 1997) but also due to the propensity for such systems to have a large Soret coefficient.(Wiegand, 2004a) Arguably the most fundamental understanding of thermal diffusion in condensed systems has been achieved with solid oxides, whose study is motivated by the need for precise control of glass composition in some optical devices.(Noritake et al., 2019) In the work by Noritake and coworkers, the Soret coefficient was determined in multicomponent solid oxides using molecular dynamic simulations. In the oxides without charge compensation, a linear relationship between the Soret coefficients and potential energy distributions was found. The potential energy distributions are related to activation energy.

The experimental efforts briefly reviewed in the previous paragraph have led to theoretical models. For more detail, the reader is referred to a review by Köhler and Morozov. (Köhler and Morozov. 2016) The thermal diffusion coefficient and the steady-state Soret coefficient can be predicted in ideal gas mixtures using kinetic gas theory. (Hirschfelder et al., 1954) Even in the simplest possible case of a binary mixture of spherical monatomic gases, the thermal diffusion ratio is "a very complex function of temperature, concentration, and molecular weights and depends parametrically on the force law of the molecules." (Hirschfelder et al., 1954) Moreover, Hirschfelder, Curtiss, and Bird explain that the error from the approximation used to derive an analytical expression for the thermal diffusion ratio, which is closely related to the Soret coefficient, is greater than for any other transport coefficient found using a similar approach. Another approach is grounded in thermodynamics. Thermal diffusion expressions based on thermodynamics have been developed by many researchers. (Köhler and Morozov, 2016) Some of these expressions are able to predict the behavior of simple mixtures (one phase, lacking strong intermolecular interactions) in the limit of small temperature gradients. (Köhler and Morozov, 2016; Rahman and Saghir, 2014) However, in practical systems where the Soret Effect is relevant,

temperature gradients are much larger than the range to which irreversible thermodynamics is expected to apply. Kempers used a clever approach to overcome the limitation of small temperature and concentration gradients by decoupling the kinetic component from the thermodynamic component of the model.(Kempers, 2001) This allowed him to start from equilibrium thermodynamics, although it did require using the definition of the Soret coefficient from irreversible thermodynamics. He has shown that kinetic gas theory can be combined with thermodynamics to predict Soret coefficients in liquids (and interacting gases).(Kempers, 2001) This model handles nonideality using molar properties of the components that are determined with equation of state (EOS) software. Unfortunately, Kempers reports that EOS software at the time was of insufficient accuracy due to the extreme sensitivity of the Soret coefficient to EOS values. Despite this shortcoming, reasonable agreement with many experimental Soret coefficients was found, although Kempers reports agreement with liquid hydrocarbons to be fair to poor.(Kempers, 2001) More recently, the model has been successfully applied to solid oxides.(Shimizu et al., 2018) Qualitatively, the model predicts that Soret coefficients will increase with increasing nonideality.

Although significant progress has been made in understanding and predicting Soret coefficients, both kinetic gas theory and thermodynamic models yet suffer from significant error. There also remain gaps in our understanding of thermal diffusion. For example, the direction of thermal diffusion can switch with composition of the mixture.(Kita et al., 2004) Although some qualitative hypotheses have been put forward, it is not currently possible to predict this behavior. This inhibits our ability to identify promising mixtures for use in thermogalvanic cells. Currently, thermogalvanic cells utilize materials that are either very expensive or inefficient, rendering them impractical.(Lee et al., 2014) There is an incentive to find cheaper, more energy-efficient materials to use within these devices. The process of developing an effective thermogalvanic cell would be facilitated if it were known which mixtures offered the greatest potential for this application. Therefore, an

equation is derived that relates pure component self-diffusion coefficients to the Soret coefficient.

This relationship is used in simplified form to semi-empirically examine published data with a graphical approach to understanding the role that self-diffusion-based activation energy plays in thermal diffusion.

96

97

98

99

100

101

102

103

104

105

106

107

108

109

110

111

112

113

114

115

116

117

118

119

120

The purpose of this work is to investigate a potential relationship between the activation energy of self-diffusion of the two individual parts of a binary mixture and the mixtures' resulting Soret coefficient. Our prediction is that whichever component has a greater activation energy will thermally diffuse to the cold side, while the other component will thermally diffuse in the opposite direction. The gradient in rate of thermal fluctuations results in a flux from faster thermal fluctuations (higher temperature) to slower (lower temperature). This would be expected to occur for all components in a mixture, which gets to the underlying reason why thermal diffusion is a small effect in many systems. A concentration gradient only develops due to a relative flux of the species whose difference in thermal fluctuation rate is greater. In other words, the higher activation energy component thermally diffuses to the cold side. If this turns out to be true, this would be a major breakthrough in our understanding of thermal diffusion, because it would tell us that the mobility that determines Fickian diffusion and thermal diffusion is fundamentally the same. The difference is that Fickian diffusion depends on the mean of the component mobilities (and a thermodynamic factor) and thermal diffusion depends on the relative temperature-dependence of the component mobilities, i.e. relative activation energies. The relationship between Fickian diffusivities and self-diffusivities is already well established. (Krishna and van Baten, 2005; Vrentas and Vrentas, 2007) In dilute and polymer solutions, a proportionality has been found between D_T and the self-diffusion coefficient of the solvent. (Brenner, 2006; Rauch et al., 2007) However, the idea that thermal diffusivities are related to activation energy of self-diffusion is new approach that could elucidate the aforementioned proportionality and will be applied to concentrated solutions. If the hypothesis is correct, it would mean that binary combinations could be screened separately and those with the greatest difference in self-diffusion activation energy would yield the largest concentration gradient at Soret steady state.

Methodology

- This work is entirely computational, based on data taken from the literature. The basis for including given Soret data include 1) the need to also have available self-diffusion activation energies and 2) the data was generated from simple experiments with clearly defined bounds. Only binary liquid mixtures were examined, and only data collected via the following 6 methods were used.
 - Thermal Diffusion Forced Rayleigh Scattering: Interference fringes, created by the intersection of two equal-intensity laser beams, interact with a dye to create temperature gradients whose spatial extent is defined by the varying light intensity. The Soret Effect results in the development of a concentration grating. Both the temperature and concentration gradients induce a refractive index grating that is measured by a second laser utilizing Bragg diffraction. The benefits of this technique are that it has a diffusion time on the order of milliseconds. The drawbacks are that the experiments must be run thousands of times to give accurate results. The temperature-gradient used in these experiments is on the order of $100 \,\mu\text{K}/10 \,\mu\text{m} = 0.1 \,\text{K/cm.}$ (Platten, 2006)
 - Sliding symmetrical tubes & Thermo-gravitational Columns: Two vertical concentric cylinders held at different temperatures are used to create a temperature gradient. The sample is placed between the two cylinders and the gradient is imposed horizontally. Concentration is measured using multiple sample taps along the tubes. In this method, convection is a significant part of creating the concentration gradient. However, given the dimensions of the tubes, vertical diffusion can be neglected at steady state. This method is more labor-intensive than other methods, but it is also the oldest and most well

understood.(Platten, 2006) In particular, the technique has been used to separate hydrocarbons as well as to understand how geothermal gradients affect local hydrocarbon concentrations in petroleum deposits.(Platten, 2006) The temperature-gradient used in these experiments is on the order of 1 K/0.1 cm = 10 K/cm. (Platten, 2006)

- Optical Beam Deflection: This technique is used primarily for binary liquid mixtures. The liquid is contained in a box with a temperature plate on the top and bottom, and optical glass on the sides. The plates at different temperatures impose a temperature gradient that over time will create a concentration gradient in the mixture. A laser is passed through the mixture, and the degree of refraction in the beam is used to calculate the gradient. This method is simple to set up and offers more potential applications as the temperature can be controlled more easily. However, relaxation times are very long, and getting repeated results takes a large amount of time.(Platten, 2006) The temperature-gradient used in these experiments is on the order of 1 K/0.1 cm = 10 K/cm.(Koeniger et al., 2009)
- Optical Digital Interferometry: The mixture is placed into a glass frame clamped between two highly conductive metal plates used to drive the temperature gradient. The cell is placed into an interferometer, and diffusion is measured via a complex optical arrangement involving the reflection of a He-Ne laser. This method is unique as it traces the transient path of the system over the full cross-section of the cell. (Mialdun et al., 2012) The temperature-gradient range used in these experiments is on the order of 10 K/cm. (Mialdun et al., 2012)
- Stirred Diaphragm Cells: Diaphragm cells can have a wide range of specifications and designs. In the simplest form, a diaphragm cell is composed of a sintered diaphragm in a casing. Diffusion is confined to the pores of the diaphragm, allowing for the use of large gradients measured in a short time. However, there is a significant amount of potential variance in this method, and some scientists question the reproducibility of this method.(Gordon, 1945)

- Influence of Vibrations on Diffusion in Liquids: This experiment uses the optical digital interferometry technique, but it was done onboard the international space station (ISS) under microgravity conditions. (Mialdun et al., 2012) The temperature-gradient range used in these experiments is on the order of 10 K/1 cm = 10 K/cm. (Mialdun et al., 2012)

These 6 methods were found to have a sufficient amount of available data to evaluate their reliability. Consistency among the techniques was taken as an indication of their accuracy. Possibly due to specific interactions, mixtures with a chlorine-containing compound exhibit behavior completely uncorrelated to any other data. This was true for both carbon tetrachloride and chlorobenzene. As a result, it was excluded from our data on the basis that there is some unique intermolecular interaction(s) occurring that cannot be otherwise accounted for without detailed equation of state input or some measurement of the thermodynamic factor. Herein is reported a database of Soret coefficient values that have been collected from literature reporting compilations of multiple studies as well as some original reports. This database (found in its entirety in the associated dataset)(Silverman and Hallinan Jr, 2020) includes the components and concentrations of the binary mixture, the Soret coefficient, the experimental method, and experimental conditions. In addition, this investigation required the use of the activation energy of self-diffusion for each component. This information is not widely available, and most of it had to be calculated. To achieve this, we compiled temperature-dependent self-diffusion coefficient data from a variety of sources. Then, Arrhenius plots were used in the following format:

$$ln(\mathcal{D}) = ln(\mathcal{D}_0) - \frac{E_a}{R} * \frac{1}{T}$$

The activation energy, E_a , was calculated by multiplying the magnitude of the slope of $\ln(\mathcal{D})$ versus 1/T by the gas constant, $R=0.008314\frac{\mathrm{kJ}}{\mathrm{mol\ K}}$. The self-diffusion activation energies are reported in Table 1.

Table 1. Activation energy for self-diffusion of each component included in this study.

Substance	Activation energy (kJ/mol)	95% Confidence interval	Temperature range (K)	Source
acetone	8.62	+/- 0.679	186-334	(Suárez-Iglesias et al., 2015)
benzene	12.829	+/- 0.589	283-318	(Winter, 1952)
cyclohexane	14.62	+/- 0.621	281-333	(Suárez-Iglesias et al., 2015)
decane	13.313	+/- 0.323	247-444	(Suárez-Iglesias et al., 2015)
dodecane	13.74	+/- 0.984	278-334	(Suárez-Iglesias et al., 2015)
ethanol	15.247	+/- 0.694	239-340	(Guevara-Carrion, 2009)
hexane	8.25	+/- 2.04	193-349	(2020)
IPA	24.36	+/- 2.82	298-339	(Pratt, 1975)
methanol	12.67	+/- 0.501	213-340	(Guevara-Carrion, 2009)
octadecane	16.901	+/- 0.921	301-439	(Suárez-Iglesias et al., 2015)
pentane	6.833	+/- 0.331	190-309	(Suárez-Iglesias et al., 2015)
toluene	11.27	+/- 0.285	202-379	(Suárez-Iglesias et al., 2015)
water	17.361	+/- 0.871	273-364	(Suárez-Iglesias et al., 2015)

Terms & Definitions

The complete compiled Soret data are reported in the associated dataset. (Silverman and Hallinan Jr, 2020) It includes: names of component 1 and component 2, the mole fraction of each component, the average temperature in Kelvin at which the data was collected, the Soret coefficient measurement method, and the resulting Soret coefficient in K^{-1} . The designation of component 1 and component 2 is arbitrary due to mutual counter-diffusion occurring in the binary liquid mixtures, and $D_{12} = D_{21}$. However, the designation is important because it determines the sign of the thermal diffusion coefficient, i.e. $D_{T,12} = -D_{T,21}$. Since $S_{T,12} = D_{T,12}/D_{12}$, the designation also determines the sign of the Soret coefficient. A positive Soret coefficient indicates that thermal diffusion of component 1 occurs from higher temperature to lower temperature. In other words, positive S_T indicates that component 1 concentrates at the lower temperature (and component 2 concentrates at the higher temperature due to conservation of mass). Since the mutual (Fickian) diffusion coefficient is always positive, a negative Soret coefficient indicates that the flux of component 1 due to thermal diffusion is from low to high temperature. The convention in this study was to define the components such that the weighted E_a difference (defined below)

would be positive, effectively looking at only the magnitude of weighted E_a differences. In experiments where the difference was negative (with the components as defined in the original literature report), the designation of components was switched and the sign of the Soret coefficient was changed (to account for the change in the component designation).

Results and Discussion

In order to develop a relationship between self-diffusion-based activation energies and the Soret coefficient, it is convenient to express the Soret coefficient $S_T = D_T/D_{AB}$ in terms of the thermal diffusion coefficient, D_T , and the mutual diffusion coefficient, D_{AB} . In an initially homogeneous mixture that is subjected to a temperature gradient, the only way for a concentration gradient to develop is if the diffusive flux of component A, J_A , is different from that of component B, J_B . In other words, in a binary mixture the net flux creating the concentration gradient is equal to the flux due to thermal diffusion.

225
$$J_A - J_B = 0.5(3R)^{1/2} \left[T_2^{1/2} - T_1^{1/2} \right] \left[\frac{c_A}{M_A^{1/2}} - \frac{c_B}{M_B^{1/2}} \right] = c x_A x_B D_T \nabla T$$
 (1)

All variables are defined in the definition of variables section. Thus, for 1-dimensional diffusion in the *x*-direction,

$$D_T = \frac{\Delta x}{2cx_A x_B \Delta T} (3R)^{1/2} \left[T_2^{1/2} - T_1^{1/2} \right] \left\{ \left[\left(\frac{3RT_2}{M_A} \right)^{1/2} - \left(\frac{3RT_1}{M_A} \right)^{1/2} \right] c_A - \left[\left(\frac{3RT_2}{M_B} \right)^{1/2} - \left(\frac{3RT_1}{M_B} \right)^{1/2} \right] c_B \right\}$$

229 (2)

Note that the velocity of component i at temperature j is $v_{ij} = \left(\frac{3RT_j}{M_i}\right)^{1/2}$. The self-diffusion coefficient of component i at temperature j can be considered $\mathcal{D}_{ij} = \Delta x \, v_{ij}$, such that

232
$$D_T = \frac{1}{2c_{XAXB}\Delta T} \{ [\mathcal{D}_{A2} - \mathcal{D}_{A1}] c_A - [\mathcal{D}_{B2} - \mathcal{D}_{B1}] c_B \}.$$
 (3)

233 Self-diffusion coefficients follow an Arrhenius temperature dependence.

$$234 \mathcal{D}_{ij} = \mathcal{D}_{i0}e^{-E_i/RT_j} (4)$$

235 Since $x_i = c_i/c$,

236
$$D_T = \frac{1}{2x_A x_B \Delta T} \{ \mathcal{D}_{A0} \left[e^{-E_A/RT_2} - e^{-E_A/RT_1} \right] x_A - \mathcal{D}_{B0} \left[e^{-E_B/RT_2} - e^{-E_B/RT_1} \right] x_B \}$$
 (5)

- Next, we can use the Darken relation to relate the mutual diffusion coefficient to the self-diffusion
- 238 coefficients.(Krishna and van Baten, 2005)

$$239 D_{AB} = T_h(x_B \mathcal{D}_A + x_A \mathcal{D}_B) (6)$$

- where T_h is a thermodynamic factor that accounts for deviation from ideality. It is unity in an ideal
- 241 system, which will be assumed here. Taking the mutual diffusion coefficient at some average
- 242 temperature, T,

243
$$D_{AB} = (x_B D_{A0} e^{-E_A/RT} + x_A D_{B0} e^{-E_B/RT})$$
 (7)

244 Inserting equations 5 and 7 into the Soret coefficient ratio yields

245
$$S_T = \frac{1}{2x_A x_B \Delta T} \frac{\{ \mathcal{D}_{A0} [e^{-E_A/RT_2} - e^{-E_A/RT_1}] x_A - \mathcal{D}_{B0} [e^{-E_B/RT_2} - e^{-E_B/RT_1}] x_B \}}{(x_B \mathcal{D}_{A0} e^{-E_A/RT} + x_A \mathcal{D}_{B0} e^{-E_B/RT})}.$$
 (8)

246 Rearranging

247
$$S_{T} = \frac{1}{2x_{A}x_{B}\Delta T} \frac{\left[e^{\frac{E_{A}(\frac{1}{T}-\frac{1}{T_{2}})}{2}} - e^{\frac{E_{A}(\frac{1}{T}-\frac{1}{T_{1}})}{2}}\right]x_{A}}{x_{B} + x_{A}\frac{\mathcal{D}_{B0}}{\mathcal{D}_{A0}}e^{(E_{A}-E_{B})/RT}} - \frac{\left[e^{\frac{E_{B}(\frac{1}{T}-\frac{1}{T_{2}})}{2}} - e^{\frac{E_{B}(\frac{1}{T}-\frac{1}{T_{1}})}{2}}\right]x_{B}}{x_{B}\frac{\mathcal{D}_{A0}}{\mathcal{D}_{B0}}e^{(E_{B}-E_{A})/RT} + x_{A}}}.$$
 (9)

- 248 If T_2 and T_1 are sufficiently similar, then $\frac{1}{T} \frac{1}{T_2} \cong \frac{1}{T} \frac{1}{T_1} \cong \frac{\Delta T}{2T^2}$. Using this assumption, equation A9
- 249 can be simplified to

250
$$S_T = \frac{1}{x_A x_B \Delta T} \frac{\frac{x_A}{x_B} \sinh(\frac{E_A \Delta T}{2RT^2}) - \frac{\mathcal{D}_{B0}}{\mathcal{D}_{A0}} \sinh(\frac{E_B \Delta T}{2RT^2}) e^{(E_A - E_B)/RT}}{1 + \frac{x_A \mathcal{D}_{B0}}{x_B \mathcal{D}_{A0}} e^{(E_A - E_B)/RT}}.$$
 (10)

For all Soret coefficient measurements compiled in this study $\frac{\Delta T}{2T^2}$ is small, on the order of 10^{-3} .

$$\lim_{\frac{\Delta T}{T^2} \to 0} \frac{\sinh\left(\frac{E_i \Delta T}{2RT^2}\right)}{\frac{\Delta T}{T^2}} \to \frac{E_i}{2R} \tag{11}$$

253 With these assumptions, a final exact expression for the Soret coefficient is

254
$$2x_{A}x_{B}TS_{T} = \frac{x_{A}\frac{E_{A}}{RT}D_{A0} e^{\left(\frac{-E_{A}}{RT}\right)} - x_{B}\frac{E_{B}}{RT}D_{B0} e^{\left(\frac{-E_{B}}{RT}\right)}}{x_{B}D_{A0} e^{\left(\frac{-E_{A}}{RT}\right)} + x_{A}D_{B0} e^{\left(\frac{-E_{B}}{RT}\right)}}.$$
 (12)

In the limit as the activation energy difference, $E_A - E_B$, goes to zero

$$256 \qquad \lim_{(E_A - E_B) \to 0} S_T \to \frac{1}{2x_A x_B T} \frac{\frac{x_A}{x_B} \frac{E_A}{RT} - \frac{\mathcal{D}_{B_0}}{\mathcal{D}_{A_0}} \frac{E_B}{RT}}{1 + \frac{x_A \mathcal{D}_{B_0}}{x_B \mathcal{D}_{A_0}}} = \frac{E_B}{2x_A x_B R T^2} \frac{\frac{x_A}{x_B} \frac{E_A}{E_B} - \frac{\mathcal{D}_{B_0}}{\mathcal{D}_{A_0}}}{1 + \frac{x_A \mathcal{D}_{B_0}}{x_B \mathcal{D}_{A_0}}} = \frac{1}{2x_A x_B R T^2} \frac{x_A E_A - \frac{\mathcal{D}_{B_0}}{\mathcal{D}_{A_0}} x_B E_B}{x_B + x_A \frac{\mathcal{D}_{B_0}}{\mathcal{D}_{A_0}}}.$$

$$(13)$$

For an equimolar mixture with equal \mathcal{D}_{i0} , S_T goes to zero in the limit as $E_A - E_B$ goes to zero, but it can be nonzero for unequal \mathcal{D}_{i0} and/or asymmetric mixture composition. The parametric plots of Figure 1 and Figure 2 use equation 12 to examine the effect of \mathcal{D}_{i0} ratio and composition on S_T , respectively. In Figure 1 with unequal \mathcal{D}_{i0} , the trend of the model qualitative agrees with the compiled data up to a value of $x_A E_A - x_B E_B \leq 5$. It is worth noting that the greatest weighted activation energy difference in the compiled data is 16. However, in the limit of large weighted activation energy difference, the compiled data does not appear to tend toward zero, as Figure 1 would suggest. It is interesting to note that Figure 1 was generated by incrementing the value of E_A larger and the value of E_B smaller, but large weighted activation energy difference could be achieved with finite E_B values that would not drive S_T to zero. The effect of E_B on S_T values in the limit of large weighted activation energy difference is shown in Figure 3. The derived expression does not require S_T to tend toward zero, but rather a negative value, as the compiled data demonstrates.

270
$$\lim_{(E_A - E_B) \to \infty} S_T \to -\frac{1}{2x_A x_B T} \frac{x_B}{x_A} \frac{E_B}{RT}$$
 (14)

It will be interesting to see if a minimum is observed as mixtures with yet larger self-diffusion activation energy differences are studied. Due to uncertainty in determining \mathcal{D}_{i0} values, i.e. the self-diffusion coefficient at infinite temperature $(\frac{1}{T} \to 0)$, this study focused simply on empirical correlation with weighted activation energy differences (and ratios) rather than using the exact expression derived in equation 12. It is worth pointing out that different expressions could have been chosen to relate thermal and mutual diffusion coefficients to self-diffusion coefficients, which would have resulted in a different final expression for the Soret coefficient. The expressions used here are grounded in a phenomenological understanding of continuum transport theory and have been widely used by other investigators.

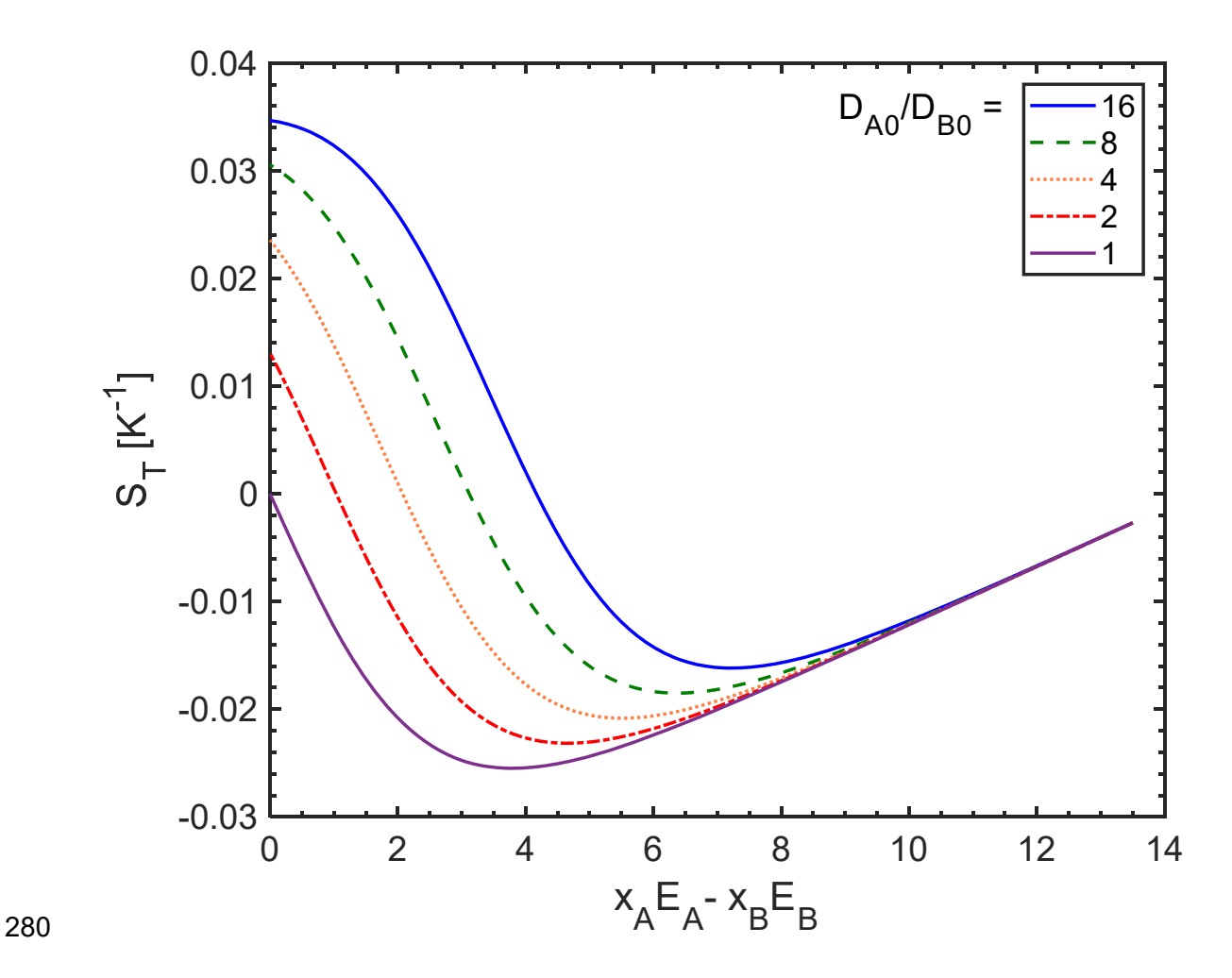


Figure 1. Parametric plot of Soret coefficient versus weighted activation energy difference for different values of the ratio of the Arrhenius pre-exponential constants for self-diffusion (noted in legend). The ratios were achieved by fixing $\mathcal{D}_{B0}=1\times 10^{-8}~cm^2/s$ and varying \mathcal{D}_{A0} . This plot was generated using equation 12 with $x_A=x_B=0.5,~T=298~K$ (i.e. RT=2.48~kJ/mol), E_A values between 28 and 14.5 kJ/mol, and E_B values between 1 and 14.5 kJ/mol.

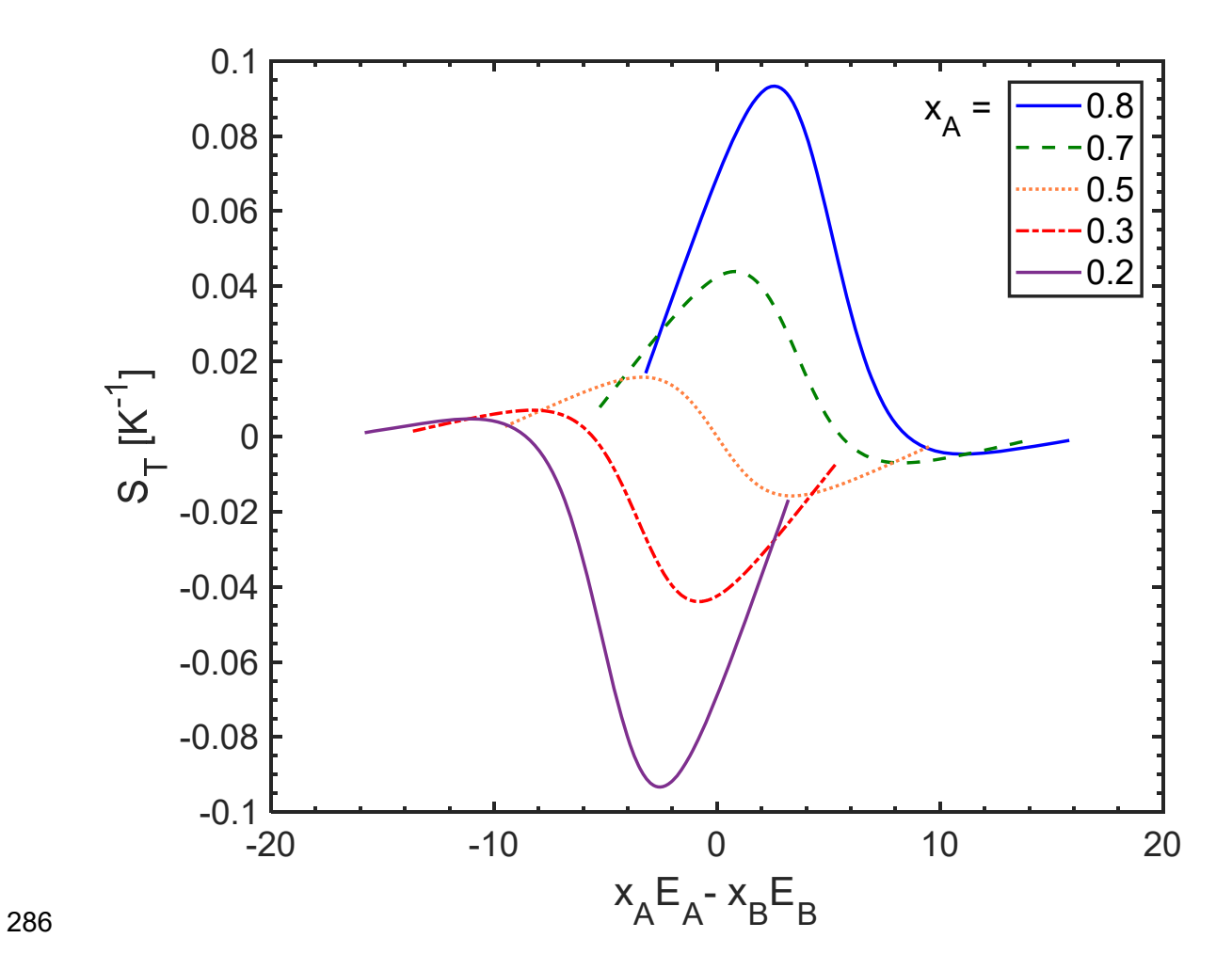


Figure 2. Parametric plot for different mixture compositions (noted in legend). This plot was generated using equation 12 with $\mathcal{D}_{A0}=\mathcal{D}_{B0}=1\times 10^{-8}\ cm^2/s$, $T=298\ K$ (i.e. $RT=2.48\ kJ/mol$), and E_A and E_B values between 1 and 20 kJ/mol. Note that $x_B=1-x_A$.

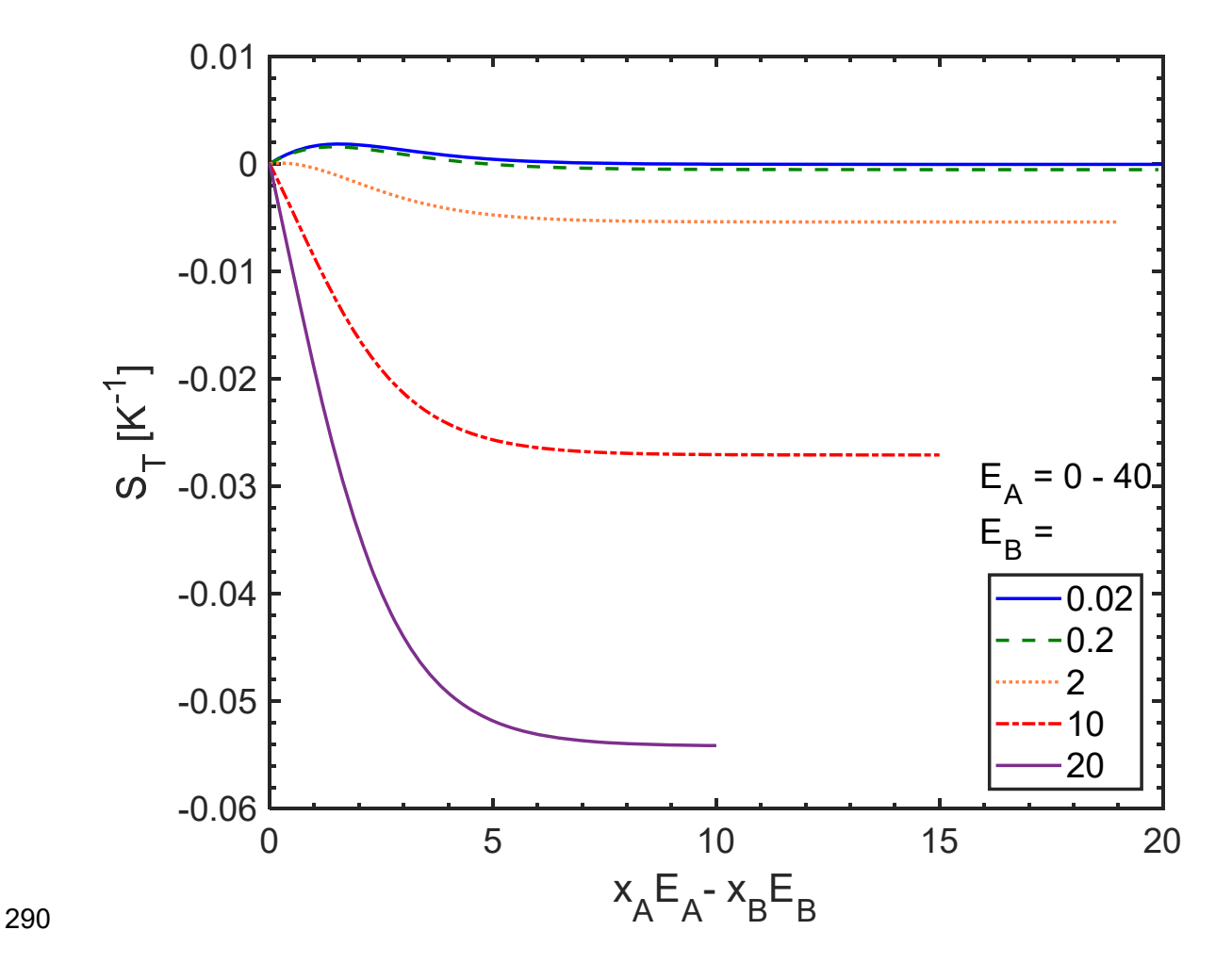


Figure 3. Parametric plot examining the effect of the self-diffusion activation energy of component B (noted in legend). This plot was generated using equation 12 with $x_A = x_B = 0.5$, T = 298~K (i.e. RT = 2.48~kJ/mol), and $\mathcal{D}_{A0} = \mathcal{D}_{B0} = 1~\times 10^{-8}~cm^2/s$. For each curve, the weighted activation energy difference was varied by changing the value of E_A between 40 to 0 E_A between 40 to 0

Motivated by this derivation, several simplified relationships between the activation energies of self-diffusion of each component in a binary mixture and the Soret coefficients of the mixtures were examined. As shown in equation 13, for small activation energy differences, similar self-diffusion prefactors, and similar composition, S_T would be expected to scale with the weighted activation energy ratio:

301
$$\frac{x_1 E_{a,1}}{x_2 E_{a,2}}$$

where x_i is the mole fraction of component i. The relationship between the compiled S_T data and the weighted activation energy ratios are presented graphically in Figure 4. This graph shows a general but weak trend that as the ratio of activation energy gets larger, the Soret coefficient tends towards a large negative value.

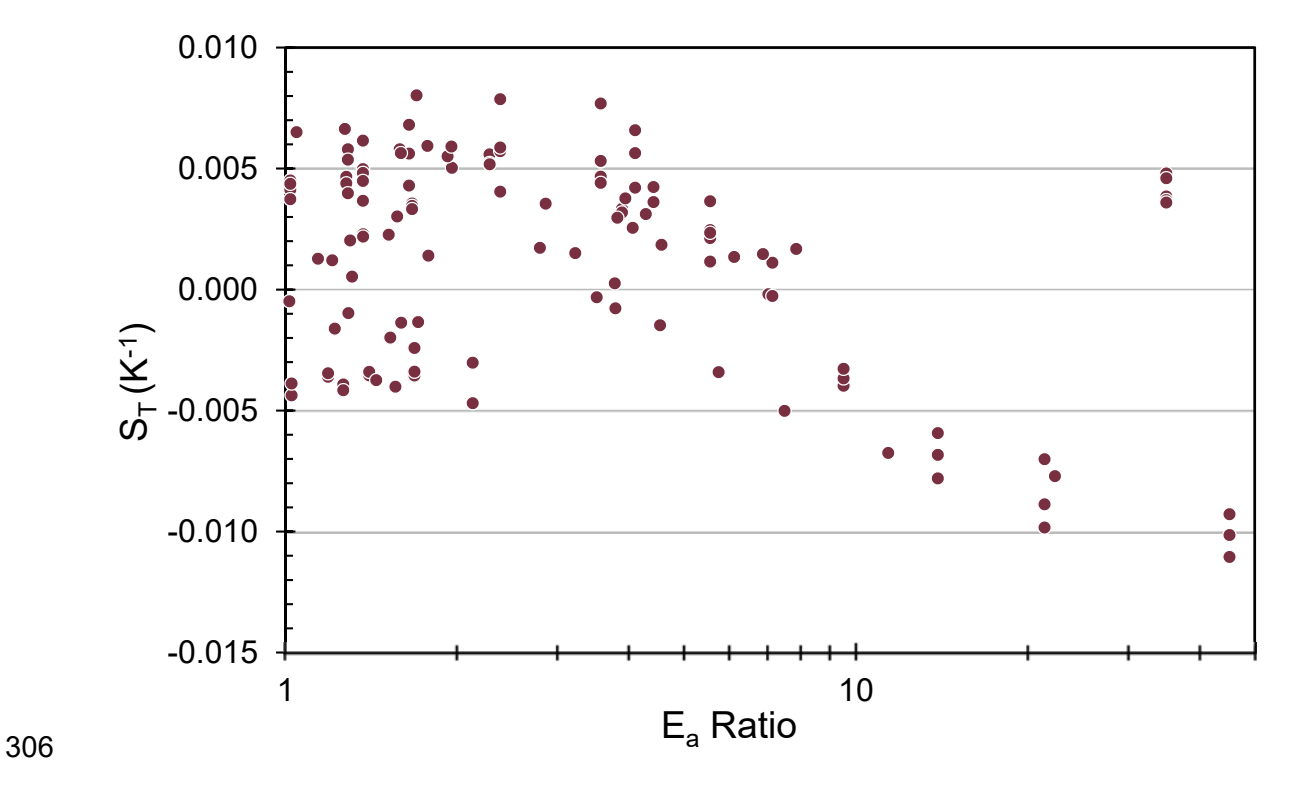


Figure 4. Soret coefficients versus mole-fraction-weighted activation energy ratio. The horizontal axis is log-scale.

By rearranging equation 13, one might expect S_T to scale with a weighted activation energy difference, as follows.

$$x_1 E_{a,1} - x_2 E_{a,2}$$

The plot of Soret coefficients versus this weighted activation energy difference is presented in Figures 5a and 5b. A parabolic relationship is apparent in Figure 5a (see dashed curve), indicating

that as weighted E_a difference increases, the magnitude of S_T gets larger. Due to the large scatter in data for small weighted E_a difference, it is unclear if the parabolic trend is real or if rather there is a threshold weighted E_a difference above which a linear trend occurs (with negative slope). The latter behavior would be in agreement with molecular dynamic simulations of silicate liquids that found a linear relationship between S_T and E_a .(Noritake et al., 2019) It could also be rationalized if there is a minimum weighted E_a difference required for the experimental techniques to accurately detect S_T values. There is a clear trend of increasingly negative S_T values with increasing weighted E_a differences. It can be explained physically as follows. In a mixture that is initially homogeneous and exposed to a temperature gradient, net flux due to thermal diffusion is not driven by differences in the number of diffusing species (as is the case for Fickian diffusion driven by a concentration gradient), but rather it is driven by the difference in the rate of diffusive jumps in regions of different temperature. Since all diffusion coefficients follow Arrhenius behavior, this would indicate that both species would tend to diffuse from hot to cold since the rate of diffusive jumps is higher on the hot side than it is on the cold side. The flux of both species from hot to cold might occur at very early times to satisfy thermal expansion (temperature dependence of mixture density). However, at Soret equilibrium conservation of mass prevents continued flux of both species in the same direction. Furthermore, such flux would not induce a change in component concentration unless the flux of one component is different from that of the other. From a molecular perspective, the development of a concentration gradient due to thermal diffusion requires the exchange of component 1 and component 2, since an exchange of two molecules of the same species results in an indistinguishable diffusive step and no change in concentration, i.e. chemically identical molecules cannot be distinguished. Thus, differences in thermal diffusion flux, which by these arguments are driven by a gradient in the rate (as opposed to number) of diffusive steps, requires that the rate difference be greater for one component than for the other. Equation 14 predicts the trend toward negative Soret coefficient values with

315

316

317

318

319

320

321

322

323

324

325

326

327

328

329

330

331

332

333

334

335

336

337

338

increasing activation energy difference. It also can explain the large scatter observed at small activation energy differences, which is likely rooted in the more complex dependence on composition and self-diffusion coefficient pre-exponential factors that were not considered due to experimental uncertainty. In order to make apparent specific trends within a given experimental technique, the data in Figure 5a is represented in Figure 5b with the technique denoted. All techniques appear to follow a similar trend, and there are no obvious discrepancies. This validates the choice of experimental techniques to include in this compilation. As shown in Figure 5b, almost all measurements of mixtures with large weighted activation energy difference have been conducted with the optical bending technique (OBD). Thus, there is a need for Soret measurements of large-weighted-E₄difference mixtures with other techniques. This will help to determine if scatter in the data is truly smaller in the limit of large weighted E_A difference. Motivated by the apparent parabolic behavior in Figure 5a, S_T was plotted versus the square of the weighted E_a difference in Figure 6. This does not appear to result in a better correlation. However, it does accentuate the possible second-order polynomial relationship, which could be rooted in the lowest-order terms of a Taylor series representation of an exponential dependence

340

341

342

343

344

345

346

347

348

349

350

351

352

353

354

355

356

of S_T on the E_a difference.

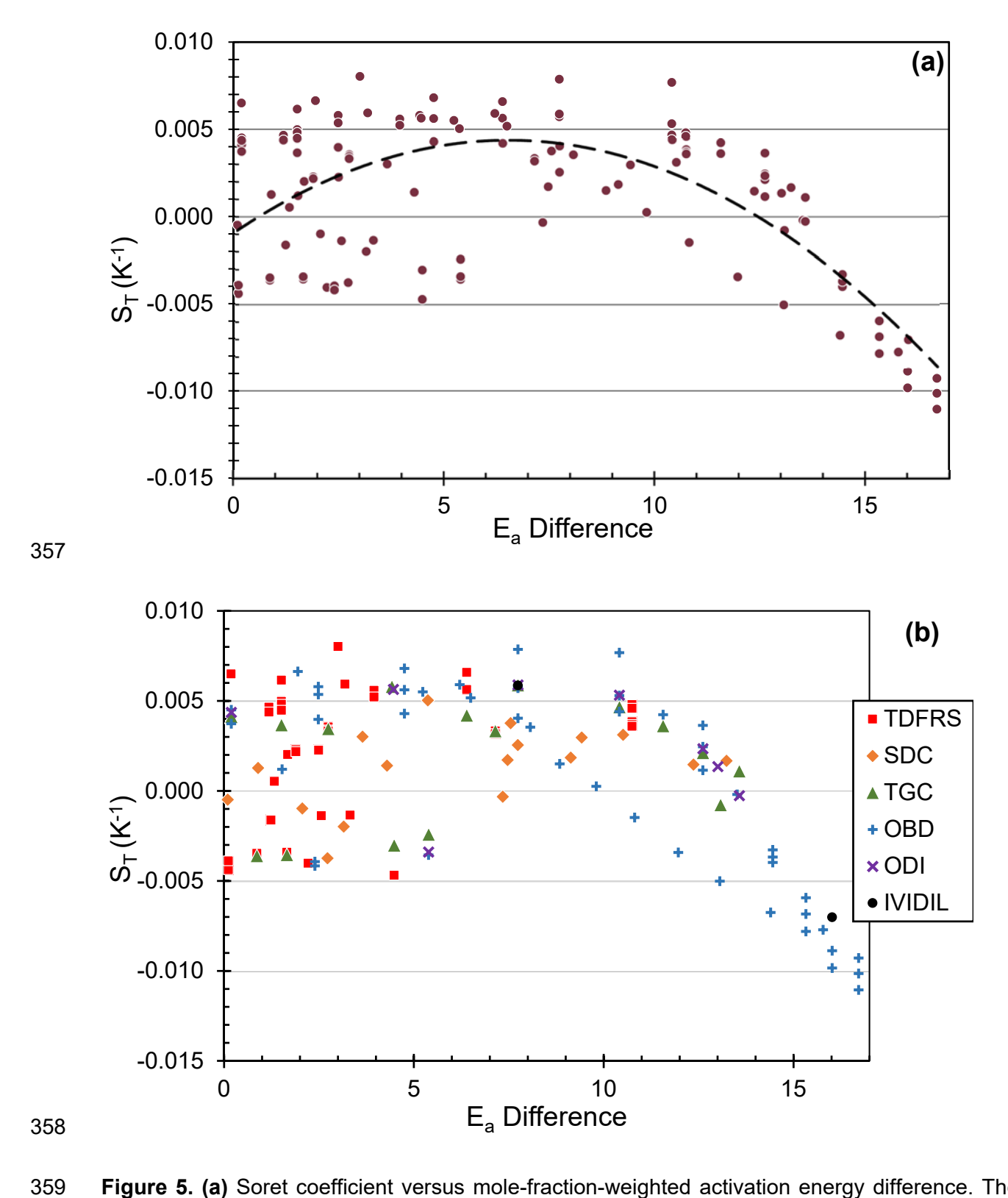


Figure 5. (a) Soret coefficient versus mole-fraction-weighted activation energy difference. The second-order polynomial fit (dashed curve) has an R-squared value of 0.52. (b) The same data

as (a) with the experimental method denoted: TDFRS – Thermal Diffusion Forced Raleigh Scattering (de Mezquia et al., 2014; Hartmann et al., 2012; Li et al., 1994; Ning et al., 2006; Platten, 2006) SDC – Stirred Diaphragm Cell (Tyrell, 1961; Wiegand, 2004b), TGC – Thermogravimetric Column (Alonso de Mezquia et al., 2014; Ecenarro et al., 1990; Mialdun et al., 2012), OBD – Optical Bending Technique (Mialdun et al., 2012), ODI – Optical Digital Interferometry (Mialdun et al., 2012), and IVIDIL – Influence of Vibrations on Diffusion in Liquids (Mialdun et al., 2012).

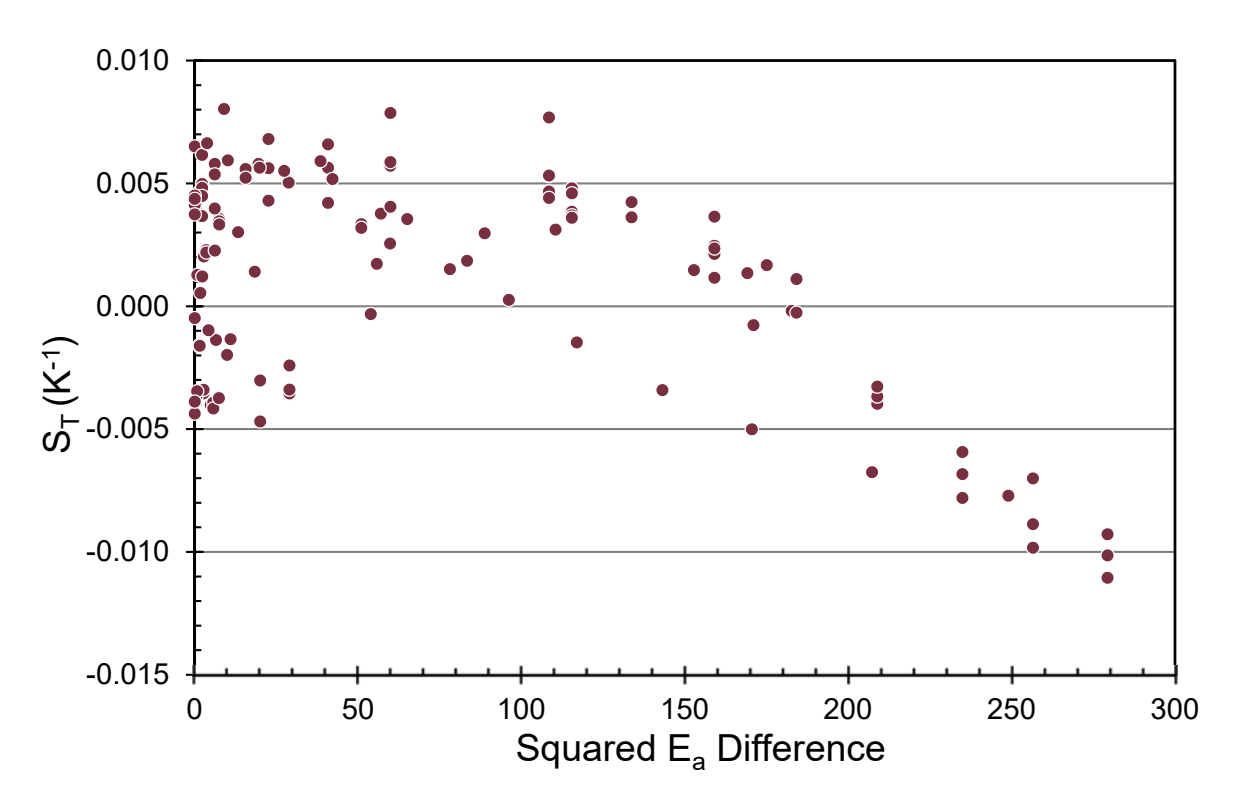


Figure 6. Weighted activation energy difference squared versus Soret coefficient.

Table 2. This table provides a summary of the Soret coefficient data. Reported are the temperature ranges over which Soret coefficients were measured, as well as the range of Soret coefficients for each binary mixture. If only one Soret coefficient is listed, the mixture had only one value reported.

Temp Range (K)		Soret Range (K ⁻¹)		Mixture		References
298		-0.00137		Acetone	Dodecane	(Hartmann et al., 2012)
298		0.00651		Acetone	Hexane	(Hartmann et al., 2012)
293	313	-0.000319	0.001853	Cyclohexane	Benzene	(Tyrell, 1961), (Wiegand, 2004b)
298		0.00803		Cyclohexane	Acetone	(Hartmann et al., 2012)
298		0.00594		Cyclohexane	Hexane	(Prigogine, 1950)
298		-0.00203		Cyclohexane	Toluene	(Hartmann et al., 2012)
300		0.00327		Decane	Pentane	(Wiegand, 2004b)
298	308.2	-0.0036	0.00356	Dodecane	Hexane	(Hartmann et al., 2012), (de Mezquia et al., 2014)
296	311.2	-0.00771	0.00664	Ethanol	Water	(Tyrell, 1961), (Wiegand, 2004b),(Koeniger et al., 2009),(Platten, 2005)
313		-0.003738	0.002971	Methanol	Water	(Tyrell, 1961)
313		-0.000479	0.00377	Methanol	Benzene	(Tyrell, 1961)
296	311.2	-0.00469	0.00659	Toluene	Hexane	(Hartmann et al., 2012), (Wiegand, 2004b), (Ecenarro et al., 1990), (Segrè et al., 1993), (Firoozabadi et al., 2000),(Kohler and Muller, 1995), (de Mezquia et al., 2014), (Li et al., 1994)
278	313	0.0036	0.0048	Toluene	Octadecane	(Ning et al., 2006)
298	308.2	-0.00134	0.00229	Toluene	Dodecane	(Hartmann et al., 2012), (de Mezquia et al., 2014)
298		0.00054		Toluene	Acetone	(Hartmann et al., 2012)
288	308	-0.01105	0.00787	Water	IPA	(Mialdun et al., 2012)

Conclusions

The graphical representation of the compiled data strongly suggests that there is a positive correlation between the magnitude of the Soret coefficient and the weighted E_a difference. Although this study does not prove that this empirical correlation is universal, it does provide sufficient evidence that future examination of an even wider range of mixtures would be warranted. This trend is a significant discovery because it could prove useful in successfully

predicting mixtures that would exhibit the largest magnitude Soret coefficient, which could impact applications such as thermally driven separations, thermogalvanic waste heat recovery, and battery efficiency related to temperature gradients. Given the variety of substances used in this study, it appears that exploring binary mixtures with increasingly large weighted E_A differences would be appropriate, as well as branching out into electrolytic and metallic substances.

Definition of variables

- c_i concentration of component i
- $c = \sum_i c_i$ total concentration of mixture
- D_{AB} Mutual diffusion coefficient in a mixture of components A and B
- \mathcal{D}_i Self-diffusion coefficient of component i
- \mathcal{D}_{i0} Pre-exponential constant for Arrhenius temperature dependence of self-diffusion
- 394 coefficient of component i
- D_T Thermal diffusion coefficient
- E_i Activation energy for self-diffusion of component i
- J_i flux of component i
- M_i molecular weight of component i
- 399 R universal gas constant
- S_T Soret coefficient
- T_i temperature of side j

402 v_{ij} – velocity of component i at temperature j403 x_i – mole fraction of component i404 ∇ – gradient

405

406

407

408

Conflict of Interest

There are no conflicts of interest to declare.

Acknowledgments

Funding for this project was provided by the IDEA grant committee at the FSU center for undergraduate research. Specifically, the funding was awarded in the form of the Scott and Ina McNichols Undergraduate Research Award. DH also acknowledges NSF Award #1751450 and Award #1804871 for partial support.

413

414

Notes and references

- 2020. Diffusion Coefficient of Hexane. Dortmund Data Bank.
- 416 Alonso de Mezquia, D., Wang, Z., Lapeira, E., Klein, M., Wiegand, S., Mounir Bou-Ali, M., 2014.
- Thermodiffusion, molecular diffusion and Soret coefficient of binary and ternary mixtures of n-hexane, n-
- dodecane and toluene. The European Physical Journal E 37, 106, 10.1140/epje/i2014-14106-2.
- Brenner, H., 2006. Elementary kinematical model of thermal diffusion in liquids and gases. Physical Review
- 420 E 74, 036306, 10.1103/PhysRevE.74.036306.
- de Mezquia, D.A., Wang, Z.L., Lapeira, E., Klein, M., Wiegand, S., Bou-Ali, M.M., 2014. Thermodiffusion,
- 422 molecular diffusion and Soret coefficient of binary and ternary mixtures of n-hexane, n-dodecane and
- 423 toluene. European Physical Journal E 37, 10.1140/epje/i2014-14106-2.
- 424 Ecenarro, O., Madariaga, J.A., Navarro, J., Santamaria, C.M., Carrion, J.A., Saviron, J.M., 1990. Fickian and
- 425 thermal diffusion coefficients from liquid thermogravitational columns. Journal of Physics: Condensed
- 426 Matter 2, 2289-2296, 10.1088/0953-8984/2/9/017.

- 427 Firoozabadi, A., Ghorayeb, K., Shukla, K., 2000. Theoretical model of thermal diffusion factors in
- 428 multicomponent mixtures. AIChE Journal 46, 892-900, 10.1002/aic.690460504.
- 429 Gordon, A.R., 1945. THE DIAPHRAGM CELL METHOD OF MEASURING DIFFUSION. Annals of the New York
- 430 Academy of Sciences 46, 285-308, 10.1111/j.1749-6632.1945.tb36172.x.
- 431 Grew, K.E., Ibbs, T.L., 1952. Thermal Diffusion in Gases. Cambridge University Press, London.
- 432 Guevara-Carrion, G., Nieto-Draghi, C., 2009. Prediction of Transport Properties by Molecular Simulation:
- 433 Methanol and Ethanol and their mixture. Cornell University, arXiv.org.
- Hartmann, S., Wittko, G., Koehler, W., Morozov, K.I., Albers, K., Sadowski, G., 2012. Thermophobicity of
- Liquids: Heats of Transport in Mixtures as Pure Component Properties. Physical Review Letters 109,
- 436 10.1103/PhysRevLett.109.065901.
- Hirschfelder, J.O., Curtiss, C.F., Bird, R.B., 1954. Molecular theory of gases and liquids. Wiley, New York.
- Jones, N., 2018. Waste Heat: Innovators Turn to an Overlooked Renewable Resource, Yale Environment
- 439 360. Yale School of the Environment, New Haven, CT.
- Kempers, L., 2001. A comprehensive thermodynamic theory of the Soret effect in a multicomponent gas,
- liquid, or solid. Journal of Chemical Physics 115, 6330-6341, 10.1063/1.1398315.
- Kita, R., Wiegand, S., Luettmer-Strathmann, J., 2004. Sign change of the Soret coefficient of poly(ethylene
- 443 oxide) in water/ethanol mixtures observed by thermal diffusion forced Rayleigh scattering. Journal of
- 444 Chemical Physics 121, 3874-3885, 10.1063/1.1771631.
- Koeniger, A., Meier, B., Koehler, W., 2009. Measurement of the Soret, diffusion, and thermal diffusion
- 446 coefficients of three binary organic benchmark mixtures and of ethanol-water mixtures using a beam
- 447 deflection technique. Philosophical Magazine 89, 907-923, 10.1080/14786430902814029.
- Köhler, W., Morozov, K.I., 2016. The Soret Effect in Liquid Mixtures A Review. Journal of Non-Equilibrium
- 449 Thermodynamics 41, 151, https://doi.org/10.1515/jnet-2016-0024.
- 450 Kohler, W., Muller, B., 1995. SORET AND MASS DIFFUSION-COEFFICIENTS OF TOLUENE N-HEXANE
- 451 MIXTURES. Journal of Chemical Physics 103, 4367-4370,
- 452 Krishna, R., van Baten, J.M., 2005. The Darken Relation for Multicomponent Diffusion in Liquid Mixtures
- of Linear Alkanes: An Investigation Using Molecular Dynamics (MD) Simulations. Industrial & Engineering
- 454 Chemistry Research 44, 6939-6947, 10.1021/ie050146c.
- 455 Lee, S.W., Yang, Y., Lee, H.-W., Ghasemi, H., Kraemer, D., Chen, G., Cui, Y., 2014. An electrochemical
- 456 system for efficiently harvesting low-grade heat energy. Nature Communications 5, 3942,
- 457 10.1038/ncomms4942.
- 458 Li, W.B., Segrè, P.N., Gammon, R.W., Sengers, J.V., 1994. Small-angle Rayleigh scattering from
- 459 nonequilibrium fluctuations in liquids and liquid mixtures. Physica A: Statistical Mechanics and its
- 460 Applications 204, 399-436, https://doi.org/10.1016/0378-4371(94)90440-5.
- 461 Malik, M.I., Pasch, H., 2016. Field-flow fractionation: New and exciting perspectives in polymer analysis.
- 462 Progress in Polymer Science 63, 42-85, https://doi.org/10.1016/j.progpolymsci.2016.03.004.
- 463 Mentor, J.J., Torres, R., Hallinan Jr., D.T., 2020. The Soret Effect in Dry Polymer Electrolyte. Molecular
- 464 Systems Design & Engineering, 10.1039/C9ME00145J
- Messaud, F.A., Sanderson, R.D., Runyon, J.R., Otte, T., Pasch, H., Williams, S.K.R., 2009. An overview on
- 466 field-flow fractionation techniques and their applications in the separation and characterization of
- polymers. Progress in Polymer Science 34, 351-368, https://doi.org/10.1016/j.progpolymsci.2008.11.001.
- Mialdun, A., Yasnou, V., Shevtsova, V., Königer, A., Köhler, W., Alonso de Mezquia, D., Bou-Ali, M.M., 2012.
- 469 A comprehensive study of diffusion, thermodiffusion, and Soret coefficients of water-isopropanol
- 470 mixtures. The Journal of Chemical Physics 136, 244512, 10.1063/1.4730306.
- Ning, H., Buitenhuis, J., Dhont, J.K.G., Wiegand, S., 2006. Thermal diffusion behavior of hard-sphere
- 472 suspensions. Journal of Chemical Physics 125, 10.1063/1.2400860.

- 473 Noritake, F., Kishi, T., Yano, T., 2019. Relationship between Soret coefficient and potential energy
- distribution in silicate liquids: A molecular dynamics study. Journal of Non-Crystalline Solids 525, 119672,
- 475 https://doi.org/10.1016/j.jnoncrysol.2019.119672.
- 476 Platten, J.K., 2005. The Soret Effect: A Review of Recent Experimental Results. Journal of Applied
- 477 Mechanics 73, 5-15, 10.1115/1.1992517.
- 478 Platten, J.K., 2006. The Soret effect: A review of recent experimental results. Journal of Applied
- 479 Mechanics-Transactions of the ASME 73, 5-15, 10.1115/1.1992517.
- Platten, J.K., Bou-Ali, M.M., Costeseque, P., Dutrieux, J.F., Kohler, W., Leppla, C., Wiegand, S., Wittko, G.,
- 481 2003. Benchmark values for the Soret, thermal diffusion and diffusion coefficients of three binary organic
- 482 liquid mixtures. Philosophical Magazine 83, 1965-1971, 10.1080/0141861031000108204.
- Pratt, K.W., WA, 1975. The mutual diffusion coefficient for binary mixtures of water and the isomers of
- 484 propanol. The Royal Society, https://doi.org/10.1098/rspa.1975.0031.
- 485 Prigogine, e.a., 1950. Physica B,
- 486 Rahman, M.A., Saghir, M.Z., 2014. Thermodiffusion or Soret effect: Historical review. International Journal
- 487 of Heat and Mass Transfer 73, 693-705, 10.1016/j.ijheatmasstransfer.2014.02.057.
- Rauch, J., Hartung, M., Privalov, A.F., Köhler, W., 2007. Correlation between thermal diffusion and solvent
- self-diffusion in semidilute and concentrated polymer solutions. The Journal of Chemical Physics 126,
- 490 214901, 10.1063/1.2738467.
- 491 Segrè, P.N., Gammon, R.W., Sengers, J.V., 1993. Light-scattering measurements of nonequilibrium
- 492 fluctuations in a liquid mixture. Physical Review E 47, 1026-1034, 10.1103/PhysRevE.47.1026.
- 493 Shimizu, M., Matsuoka, J., Kato, H., Kato, T., Nishi, M., Visbal, H., Nagashima, K., Sakakura, M.,
- Shimotsuma, Y., Itasaka, H., Hirao, K., Miura, K., 2018. Role of partial molar enthalpy of oxides on Soret
- 495 effect in high-temperature CaO-SiO2 melts. Scientific Reports 8, 15489, 10.1038/s41598-018-33882-1.
- 496 Silverman, M., Hallinan Jr, D., 2020. Data for: The relationship between self-diffusion activation energy
- and Soret coefficient in binary liquid mixtures, Mendeley Data.
- 498 Suárez-Iglesias, O., Medina, I., Sanz, M.d.I.Á., Pizarro, C., Bueno, J.L., 2015. Self-Diffusion in Molecular
- 499 Fluids and Noble Gases: Available Data. Journal of Chemical & Engineering Data 60, 2757-2817,
- 500 10.1021/acs.jced.5b00323.
- Tyrell, H.J.V., 1961. Diffusion and heat flow in liquids. Butterworth, London.
- VanBatten, C., Hoyos, M., Martin, M., 1997. Thermal field-flow fractionation of colloidal materials:
- Methylmethacrylate-styrene linear di-block copolymers. Chromatographia 45, 121-126,
- Vining, C.B., 2009. An inconvenient truth about thermoelectrics. Nature Materials 8, 83-85,
- 505 10.1038/nmat2361.
- Vrentas, J.S., Vrentas, C.M., 2007. Restrictions on Friction Coefficients for Binary and Ternary Diffusion.
- 507 Industrial & Engineering Chemistry Research 46, 3422-3428, 10.1021/ie061593a.
- 508 Wiegand, S., 2004a. Thermal diffusion in liquid mixtures and polymer solutions. Journal of Physics-
- 509 Condensed Matter 16, R357-R379, 10.1088/0953-8984/16/10/r02.
- 510 Wiegand, S., 2004b. Thermal diffusion in liquid mixtures and polymer solutions. Journal of Physics:
- 511 Condensed Matter 16, R357-R379, 10.1088/0953-8984/16/10/r02.
- 512 Winter, I.G.E.R.S., 1952. J. Chem. Soc., 1145,
- 513 Yu, B., Duan, J., Li, J., Xie, W., Jin, H., Liu, R., Wang, H., Huang, L., Hu, B., Zhou, J., 2019. All-Day
- 514 Thermogalvanic Cells for Environmental Thermal Energy Harvesting. Research 2019, 2460953,
- 515 10.34133/2019/2460953.